

## A Raman Spectroscopy Study of the Separation of Hydrofluorocarbons Using Zeolites

Michael K. Crawford,<sup>\*,†</sup> Kerwin D. Dobbs,<sup>†</sup> Robert J. Smalley,<sup>†</sup> David R. Corbin,<sup>†</sup> Nicholas Maliszewskyj,<sup>‡</sup> Terrence J. Udovic,<sup>‡</sup> Richard R. Cavanagh,<sup>‡</sup> John J. Rush,<sup>‡</sup> and Clare P. Grey<sup>§</sup>

DuPont Company, E356/209, Wilmington, Delaware 19880-0356, National Institute of Standards and Technology, Gaithersburg, Maryland 20899, and Department of Chemistry, SUNY at Stony Brook, Stony Brook, New York 11794-3400

Received: August 5, 1998; In Final Form: November 23, 1998

Hydrofluorocarbons (HFCs), such as HFC-134a (CF<sub>3</sub>CFH<sub>2</sub>), are replacing chlorofluorocarbons (CFCs) in many applications because of their low ozone depletion potentials. The more complex chemical syntheses of HFCs, however, may not provide the molecular species desired with sufficient purity, leading to the need to separate reaction products. An important example is provided by the separation of the isomers HFC-134a and HFC-134 (CF<sub>2</sub>HCF<sub>2</sub>H) over the faujisitic zeolite NaX (Na<sub>86</sub>Al<sub>86</sub>Si<sub>106</sub>O<sub>384</sub>). An understanding of the fundamental mechanism controlling this separation involves the unusual aspect that HFC-134 can exist as either a trans or gauche conformer; a key factor is that the trans conformer is nonpolar whereas the gauche conformer is highly polar. Here we report the results of a Raman scattering study which show the *trans-gauche* population ratio for HFC-134 adsorbed on NaX is decreased as much as 20-fold compared to the gas phase. Furthermore, the conformational ratio changes with HFC loading, the polar gauche conformer being more highly favored at low loading where the HFC-134a/HFC-134 separation factor is maximum. These observations thus demonstrate that the efficiency of this HFC separation is directly related to the HFC-134 *trans-gauche* population distribution on the zeolite surface.

## Introduction

The efficacy of zeolites for the separation of molecules<sup>1</sup> relies upon differences in molecule size, shape, or molecule–zeolite interactions. Here we are concerned with the separation of HFC-134a from its isomer HFC-134, which has been demonstrated using differential surface adsorption on X or Y zeolites.<sup>2</sup> HFC-134a is an important refrigerant that has replaced CFC-12 (CF<sub>2</sub>Cl<sub>2</sub>) in a number of applications. This separation is a consequence of the larger heat of adsorption of HFC-134 on NaX (Table 1), rather than a result of a difference in molecular size or shape. At low loading (less than one HFC molecule per supercage), the heat of adsorption for HFC-134 is 12–15 kJ mol<sup>-1</sup> larger than that of HFC-134a, whereas at high loading (four or more HFC molecules per supercage), the heat of adsorption for HFC-134 decreases to a value only 2–3 kJ mol<sup>-1</sup> greater than that of HFC-134a.<sup>3</sup> This decrease in heat of adsorption leads to a decrease in separation factor at high loading<sup>3</sup> (Table 1).

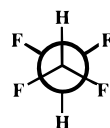
In the gas phase, HFC-134a exists as a single distinguishable staggered conformer (C<sub>s</sub> point group symmetry), corresponding to any of the three equivalent minima in its torsional potential energy surface. HFC-134a has a permanent electric dipole moment<sup>4</sup> of 1.8 D. In contrast, HFC-134 exists as one of two distinguishable staggered conformers, a trans (C<sub>2h</sub> symmetry) or gauche (C<sub>2</sub> symmetry) conformer, as shown in the following

TABLE 1: Experimental Isothermic Heats of Adsorption and Separation Factors for HFC-134A and HFC-134 on Zeolite NaX and Theoretical Binding Enthalpies for These HFCs and One or Two Na Cations

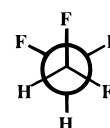
measured isothermic heat of adsorption <sup>a</sup> (kJ mol <sup>-1</sup> )		separation factor <sup>b</sup>	ab initio binding enthalpy (kJ mol <sup>-1</sup> )	
HFC-134a	HFC-134		HFC-134a	HFC-134 trans    gauche
Zero Loading			Single Na Site	
65	78	8.1	80	69    88.7
Two HFCs/Supercage			Double Na Site	
63.5	71	5.6	Unstable	69.5    80.8
Four HFCs/Supercage				
62	65	4.4		

<sup>a</sup> Isothermic heats of adsorption from ref 3. <sup>b</sup> The separation factor is defined as  $\alpha = (X_{134}Y_{134a})/(Y_{134}X_{134a})$ , where  $X_i$  is the mole fraction of HFC-*i* on the zeolite surface and  $Y_i$  is the mole fraction in the gas phase.<sup>1</sup> Data are from ref 3.

Newman projection diagrams.



Trans



Gauche

The trans conformer does not have an electric dipole moment, while the gauche conformer has a moment of 2.8 D.<sup>4,5</sup> The trans

<sup>†</sup> DuPont.  
<sup>‡</sup> NIST.  
<sup>§</sup> SUNY.

conformer is more stable (by 4.4 kJ mol<sup>-1</sup>) than the gauche conformer in the gas phase.<sup>6</sup> The potential energy barriers for internal rotation in fluorinated ethanes in the gas phase<sup>7</sup> are on the order of 12–16 kJ mol<sup>-1</sup>, which leads to rapid (10<sup>-10</sup> s) thermally activated conformational interconversion at 300 K.

The existence of two conformers of HFC-134 with very different electric dipole moments suggests the following possible origin for the decrease in separation factor with HFC loading on NaX. Since molecular properties such as electric dipole and quadrupole moments contribute to the heats of adsorption,<sup>1</sup> and these properties can depend dramatically upon molecular conformations,<sup>8</sup> a loading dependence of the conformer population ratio could change the separation factor. In fact, the experimental heats of adsorption for molecules with distinguishable conformations should be an average over both the surface conformer and adsorption site population distributions. Thus experimental determination of adsorbate conformations is central to the understanding of adsorption enthalpies and can provide important insights into the choice of substrates for separations.

Fluorinated ethanes such as HFC-134a and HFC-134 have been studied in the gas and liquid phases by techniques such as microwave, infrared, and Raman spectroscopy.<sup>6,8–11</sup> In particular, the last two techniques can readily distinguish different conformers in condensed phases,<sup>6,8</sup> directly determining the influence of the local molecular environment upon the relative conformational stability. In zeolites, Raman spectroscopy is the preferred technique for this purpose because the zeolite framework vibrations have fairly small Raman scattering cross sections,<sup>12</sup> allowing the vibrational spectra of the adsorbed HFCs to be easily observed. In contrast, infrared techniques suffer from strong absorption<sup>13</sup> due to the zeolite lattice vibrations in the spectral region below 1200 cm<sup>-1</sup>, where much of the HFC conformational information is found.<sup>6</sup> We therefore chose Raman scattering as our primary experimental method for determination of the HFC conformations.

## Experimental Section

**Sample Preparation.** The NaX used in these studies was Alpha or Aldrich 13X with the composition Na<sub>86</sub>Al<sub>86</sub>Si<sub>106</sub>O<sub>384</sub>. The NaX samples were dehydrated for 24 h at a temperature of 373 or 673 K in a vacuum. Verification of dehydration at the lower temperature was accomplished by comparing the weight loss after this treatment with that of the same material heated to 673 K in a TGA under N<sub>2</sub> atmosphere. (The low dehydration temperature was found to significantly decrease the amount of sample fluorescence during the Raman measurements.) The dehydrated NaX samples were exposed to 1 atm of HFC-134 gas and allowed to equilibrate for 24 h. The amount of adsorbed HFC in the highly loaded sample was then determined by prompt  $\gamma$  neutron activation analysis<sup>14,15</sup> (PGNAA), yielding an average value of four HFC-134 molecules per supercage. The HFC concentration in the low loading sample was determined from the pressure drop over a calibrated vacuum line and was consistent with that obtained from the weight gain after HFC adsorption. The dehydrated samples of NaX, which were used as controls for both the Raman and neutron measurements were also measured<sup>15</sup> by PGNAA and found to contain between 0.9 and 3 H atoms per supercage, present either as H<sub>2</sub>O or as framework hydroxyl groups.

**Raman Spectroscopy.** Data were obtained with a Raman microscope coupled to a two-stage monochromator system and a liquid N<sub>2</sub> cooled CCD detector. The 5145 Å line of an Ar ion laser was used as the excitation source and the power at the sample was 100–200 mW. Low-temperature measurements

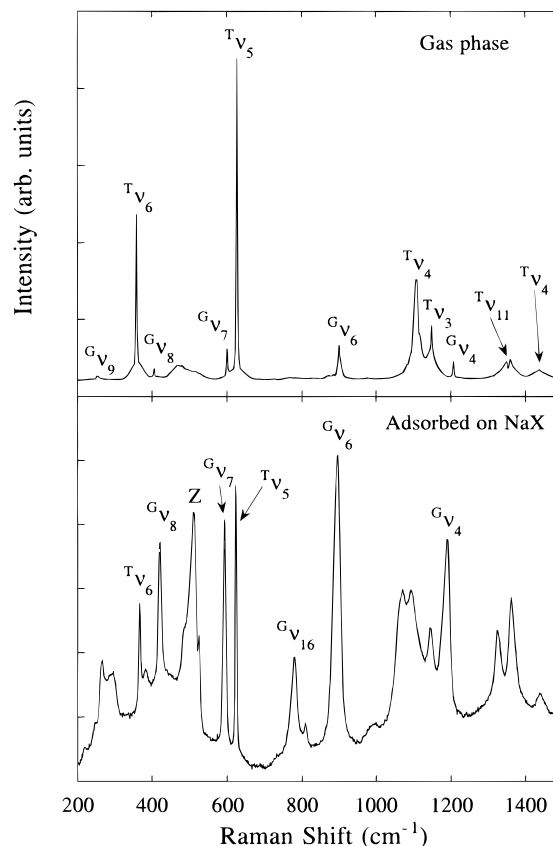


**Figure 1.** Raman spectra for HFC-134 in the gas phase (1 atm pressure) (top) and adsorbed on the zeolite NaX at a loading of four HFC-134 molecules per supercage (bottom). In the lower spectrum the peak labeled “Z” is assigned as a zeolite vibration. HFC-134 vibrational assignments are from ref 6, and the superscripts “T” and “G” designate vibrations assigned to the trans and gauche conformers, respectively. Note the large increase in the relative intensities of the gauche vibrations for the adsorbed HFC.

were made by placing the sample capillary on the coldfinger of a He flow cryostat.

**Ab Initio Density Functional Theory Calculations.**<sup>16</sup> The density functional theory calculations were performed with the Gaussian 94 program on a Cray 90 computer. The basis sets<sup>17</sup> were the local spin density optimized Gaussian basis sets DZVP. All optimized geometries and vibrational frequencies (used to determine zero-point energies and vibrational thermal corrections) were determined at the B3LYP energy level.

## Results and Discussion

In Figure 1 we show Raman spectra<sup>18,19</sup> of HFC-134 in the gas phase and adsorbed on NaX. The vibrational frequencies of the adsorbed species are only slightly shifted with respect to those observed in the gas phase, demonstrating that the adsorbed molecules still adopt staggered conformations, although the bands assigned to the gauche conformer are considerably broadened compared to the instrumental resolution. More striking, however, is the observation that the conformer population distribution is very different for the adsorbed HFC compared to the gas-phase HFC (Figure 1 and Table 2). The adsorbed species show a dramatic increase in the fraction of polar gauche HFC-134 compared to the case of the gas phase. The presence of a large fraction of the polar gauche conformer will elevate the measured<sup>3</sup> adsorption enthalpy of HFC-134.

It is also important to see if the conformer distribution is a function of HFC-134 loading, as is the adsorption enthalpy.<sup>3</sup> In

**TABLE 2: Integrated Vibrational Band Intensity Ratios for HFC-134 in the Gas Phase and Adsorbed on NaX, Measured by Raman Spectroscopy,<sup>a</sup> and the Conformer Population Ratios Estimated from the *ab Initio* Free Energy Differences<sup>b</sup>**

	gas phase	2 HFC/supercage	4 HFC/supercage	
			300 K	10 K
$I_T(620\text{ cm}^{-1})/I_G(595\text{ cm}^{-1})^c$	9.5(1.1)	0.30(3)	0.62(1)	0.59(8) 0.7(6) <sup>d</sup>
$I_T(358\text{ cm}^{-1})/I_G(405\text{ cm}^{-1})^c$	10.5(1.2)		0.33(3)	
<i>ab initio</i> <i>trans/gauche</i> population ratios <sup>b</sup> (at 300 K)	7.2		0.006 (single Na site) 0.82 (double Na site)	

<sup>a</sup> The Raman integrated intensity ratios  $I_T/I_G$  are related to the true population ratios  $N_T/N_G$  by an unknown factor whose value depends on the Raman scattering cross sections for the vibrations with intensities  $I_T$  and  $I_G$ . The ratios for two pairs of vibrations are given for the gas phase and the more highly loaded NaX sample, where the members of each pair have been assigned to similar vibrational modes for the *trans* or *gauche* conformer and would therefore be expected to have similar Raman scattering cross sections. The two ratios decrease by slightly different factors upon binding to NaX, which suggests that the Raman polarizabilities for the individual vibrations may be altered by interaction with the Na cations. This effect is small, however, compared to the average change due to surface binding. Uncertainties in the last digit(s) of the experimental ratios are given in parentheses. <sup>b</sup> The conformational population ratios at thermal equilibrium satisfy the relationship  $N_T/N_G = e^{-\Delta G/RT}$ , where  $N_i$  is the number of molecules with conformation  $i$ ,  $\Delta G$  is the Gibbs free energy change associated with the conformational transition,  $R$  is the gas constant, and  $T$  is the absolute temperature.<sup>8</sup> The *ab initio* population ratios were calculated from the values of  $\Delta G$  determined by the calculations. <sup>c</sup> Determined from the intensity ratio of Raman vibrations at  $620\text{ cm}^{-1}$  ( $\nu_5$ ) and  $595\text{ cm}^{-1}$  ( $\nu_7$ ). <sup>d</sup> Determined from inelastic neutron scattering measurements (see, for example, ref 19). <sup>e</sup> Determined from the intensity ratio of Raman vibrations at  $358\text{ cm}^{-1}$  ( $\nu_6$ ) and  $405\text{ cm}^{-1}$  ( $\nu_3$ ).

Figure 2 we compare spectra for NaX samples with different HFC-134 loadings: two HFC molecules per supercage and four HFC molecules per supercage. The fraction of polar *gauche* conformer decreases by a factor of 2 at the higher loading, which is consistent with the observed<sup>3</sup> decrease in heat of adsorption. Thus, the efficiency of the separation can be directly correlated with the fraction of polar *gauche* conformer present on the zeolite surface. In Table 2 we also give the *trans/gauche* ratio for the highly loaded sample measured at low temperature (10 K) using Raman and neutron scattering. These measurements demonstrate that the *trans/gauche* ratio is nearly temperature independent, which implies that the adsorbed conformers are not in rapid thermal equilibrium, as they are in the gas phase. This observation effectively rules out the presence of any significant quantities of “free” HFC-134 in the zeolite supercage and suggests that the *trans/gauche* ratio is determined by the nature of the binding site.

These experimental results naturally lead to the question of why the HFC-134 conformer distribution changes with loading. One possible explanation is that HFC–HFC interactions, which will become increasingly important as the number of HFC molecules per supercage increases, begin to influence the distribution. The enthalpy differences<sup>6</sup> for the *trans* and *gauche* conformers of HFC-134 in the gas and liquid phases are 4.4 and 1.5  $\text{kJ mol}^{-1}$ , respectively, suggesting that increasing the HFC density stabilizes the *gauche* conformer more than the *trans* conformer, a trend opposite to that which we observe in the zeolite. We have therefore considered a second possibility in some detail, the presence of two specific types of HFC binding site.

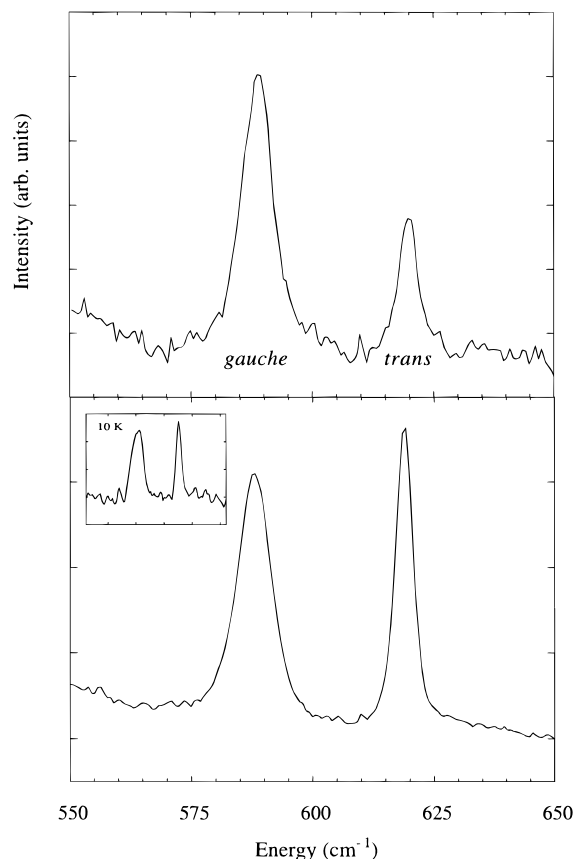


**Figure 2.** Raman spectra of HFC-134 adsorbed on NaX at low (top) or high (bottom) loading. Low loading corresponds to two molecules per supercage, and high, to four molecules per supercage. The spectrum of the highly loaded sample measured at a temperature of 10 K appears in the inset. Only the  $\nu_5$  vibration of the *trans* conformer and the  $\nu_7$  vibration of the *gauche* conformer are shown. Both vibrations have been assigned to  $\text{CF}_2$  wags.<sup>6</sup> These data suggest that the vibrational frequencies and line widths associated with molecules bound to either one or two Na cations are similar.

If we assume the HFC-134 molecules in the zeolite are distributed over two types of binding site, and these binding sites have different affinities for the *trans* and *gauche* conformers, then the measured conformational population ratios would reflect the distribution of HFC-134 molecules over these sites. If the lowest energy binding sites that are initially populated have high selectivity for the *gauche* conformer, and higher energy sites with a lower selectivity for the *gauche* conformer are populated at higher HFC loading, the result would be an increased fraction of *trans* conformer at high loading. In place of a direct experimental identification of these binding sites, we have performed *ab initio* quantum mechanical calculations to explore the properties of two possible sites.

A simplifying assumption in the calculations is that the only HFC–zeolite interactions are those between the adsorbed molecules and the extraframework Na cations. *Ab initio* density functional theory methods<sup>16,17</sup> can then be used to calculate the binding enthalpies of bare Na cations to the HFC-134a and HFC-134 molecules. We have therefore used this approach to model two binding sites: a single bare Na cation interacting with an HFC molecule or two bare Na cations interacting with an HFC molecule. The latter type of site was suggested by the results of a recent X-ray diffraction study<sup>20</sup> of HFC-134 adsorbed on the closely related zeolite NaY ( $\text{Na}_{52.8}\text{Al}_{53.6}\text{Si}_{138.4}\text{O}_{384}$ ), where two-thirds of the HFC-134 molecules were bound to two Na cations in site II and site III positions, one at either end of the molecule. Since NaX has more Na cations per supercage than



NaY,<sup>1,21</sup> and both site II and site III are occupied, similar double Na binding sites could be present. We have also measured the Raman spectrum of HFC-134 adsorbed on NaY at high loading and observed a Raman intensity ratio for the 620 and 595 cm<sup>-1</sup> vibrations of 0.9(2), comparable (within error) to that in NaX at comparable loading (Table 2), supporting the assumption that the binding sites in the two zeolites are related.

The results of these calculations are summarized in Table 1. The calculated binding enthalpy for HFC-134a and a single Na cation is larger than the measured adsorption enthalpy; we attribute this to the fact that the calculations do not include the effects of the zeolite framework. These effects include the screening of the extraframework cation charges by the framework oxygen anions, which will reduce the electrostatic binding energies; specific interactions such as hydrogen-bond formation between the HFCs and the oxygen anions of the framework, which will increase the binding energies; and nonspecific adsorbate–framework interactions such as London dispersion forces and short-range repulsion,<sup>1</sup> which will respectively increase or decrease the binding energies.

The calculated binding enthalpies for trans or gauche HFC-134 with a single Na cation (Table 1) are less or greater than the measured binding enthalpy for HFC-134 (at low loading), respectively. For an isolated HFC-134 molecule, the calculations predict the trans conformer to have the lowest energy by 4.9 kJ mol<sup>-1</sup>, in fairly good agreement with experiment<sup>6</sup> and previous calculations.<sup>22</sup> More important, however, are the predictions that the HFC-134 gauche conformer will bind most strongly to an extraframework Na cation on the zeolite surface, the trans conformer will bind most weakly, and HFC-134a will have a binding strength intermediate to the two conformers of HFC-134. Thus single Na cation binding sites could provide a basis for the HFC separation at low loading. If only single Na binding sites are present, however, we would expect the adsorption enthalpy (and conformer ratio) to be relatively constant with loading. Since this is not consistent with our observations, we now consider the second type of HFC binding site.

The ab initio calculations for a binding geometry in which two Na cations interact with a single HFC-134 molecule, one at each end, yield a gauche binding enthalpy greater than that of the trans conformer (Table 1), but the enthalpy difference is half as large as that found for HFC-134 bound to a single cation. This result is qualitatively understandable in terms of the ion–molecule electrostatic interactions, since the bidentate geometry will be less favorable for the ion–dipole interaction, whereas it is more favorable for the ion–quadrupole interaction. Further, the quadrupole strength<sup>23</sup> of trans HFC-134 is 50% larger than that of gauche HFC-134 (estimated using the quadrupole moment tensors predicted by the ab initio calculations), which will lead to a larger electric quadrupole contribution to the binding strength for the trans conformer. Thus increased occupancy of double Na binding sites at higher HFC-134 loadings would lead to a larger trans population, a decreased binding enthalpy, and consequently a less favorable separation from HFC-134a. We cannot find a similar stable bound configuration for an HFC-134a molecule and two Na cations, suggesting that single cation binding sites will dominate for that HFC at all loadings. This finding might explain the more homogeneous adsorption isotherm<sup>3</sup> of HFC-134a on NaX.

The larger fraction of HFC-134 molecules bound to two Na cations at higher loading levels could reflect an increased concentration of Na cations in the NaX supercage. The HFC–Na electrostatic interactions are apparently strong enough to induce Na cations from sites outside the supercage to migrate

to sites within the supercage, as demonstrated by an X-ray diffraction study of HFC-134 in zeolite NaY.<sup>20</sup> Furthermore, electrostatic screening of Na cation charges by intervening HFC-134 molecules will also reduce the magnitude of repulsive Na–Na interactions and permit higher Na concentrations to exist within the supercage.

These experimental and theoretical results illustrate the key role of molecular conformations in determining surface binding enthalpies for HFCs (and other molecules) in zeolites, and we therefore suggest that experimental separation strategies must consider possible effects of conformational changes of the adsorbate molecules. This is certainly true when molecules are to be separated on the basis of polarity and should be considered whether the separation is to be accomplished using molecular sieves, polymeric membranes, or other types of separation media. We have also shown that vibrational spectroscopy is a simple and direct means by which to determine the relative populations of different conformers on surfaces. Finally, such experiments can identify the most important terms in ion–molecule interaction potentials in zeolites.

**Acknowledgment.** The authors thank W. E. Farneth and D. Kragten (DuPont) and R. M. Lindstrom and R. L. Paul (NIST) for helpful discussions. We also acknowledge R. Balback (DuPont) and M. Ciruolo (SUNY, Stony Brook) for preparing some of the samples.

## References and Notes

- (1) Breck, D. W. *Zeolite Molecular Sieves*; Wiley-Interscience: New York, 1974.
- (2) Grey, C. P.; Corbin, D. R. *J. Phys. Chem.* **1995**, *99*, 16821.
- (3) Myers, A. L.; Gorte, R. J.; Savitz, S.; Huber, R.; Corbin, D. R.; Grey, C. P. Unpublished data.
- (4) Meyer, C. W.; Morrison, G. J. *J. Phys. Chem.* **1991**, *95*, 3860.
- (5) Mukhtarov, A.; Kuliev, V. A. *Izv. Akad. Nauk. SSSR, Ser. Fiz.-Tekh.* **1970**, *12*, 132.
- (6) Kalasinsky, V. F.; Anjaria, H. V.; Little, T. S. *J. Phys. Chem.* **1982**, *86*, 1351.
- (7) Brier, P. N. *J. Mol. Struct.* **1970**, *6*, 23.
- (8) Mizushima, S. *Structure of Molecules and Internal Rotation*; Academic Press: New York, 1954.
- (9) Townes, C. H.; Schawlow, A. L. *Microwave Spectroscopy*; McGraw-Hill: New York, 1955.
- (10) Klaeboe, P. *Vibr. Spectrosc.* **1995**, *9*, 3.
- (11) Xu, L.-H.; Andrews, A. M.; Cavanagh, R. R.; Fraser, G. T.; Irikura, K. K.; Lovas, F. J.; Grabow, J. U.; Stahl, W.; Crawford, M. K.; Smalley, R. J. *J. Phys. Chem.* **1997**, *101*, 2288.
- (12) Angell, C. L. *J. Phys. Chem.* **1973**, *77*, 222.
- (13) Flanigan, E. M. *Zeolite Chemistry and Catalysis*; ACS Monograph No. 171; American Chemical Society: Washington, DC, 1976; p 80.
- (14) Lindstrom, R. M. *J. Res. Natl. Inst. Stand. Technol.* **1993**, *98*, 127.
- (15) Crawford, M. K.; Corbin, D. R.; Vernooy, P. D. *Trans. Am. Nucl. Soc.* **1994**, *71*, 168.
- (16) Frisch, M. J.; Trucks, G. W.; Schlegel, H. B.; Gill, P. M. W.; Johnson, B. G.; Robb, M. A.; Cheeseman, J. R.; Keith, T.; Petersson, G. A.; Montgomery, J. A.; Raghavachari, K.; Al-Laham, M. A.; Zakrzewski, V. G.; Ortiz, J. V.; Foresman, J. B.; Cioslowski, J.; Stefanov, B. B.; Nanayakkara, A.; Challacombe, M.; Peng, C. Y.; Ayala, P. Y.; Chen, W.; Wong, M. W.; Andres, J. L.; Replogle, E. S.; Gomperts, R.; Martin, R. L.; Fox, D. J.; Binkley, J. S.; Defrees, D. J.; Baker, J.; Stewart, J. P.; Head-Gordon, M.; Gonzalez, C.; Pople, J. A. *Gaussian 94*; Gaussian, Inc.: Pittsburgh, PA, 1995.
- (17) Godbout, N.; Salahab, D. R.; Andzelm, J.; Wimmer, E. *Can. J. Chem.* **1992**, *70*, 560.
- (18) Crawford, M. K.; Corbin, D. R.; Smalley, R. J. In *Amazing Light: A Festschrift in Honor of Charles Hard Townes on His 80th Birthday*; Chao, R. Y., Ed.; Springer-Verlag: New York, 1996; Vol. 153.
- (19) Udovic, T. J.; Nicol, J. M.; Cavanagh, R. R.; Rush, J. J.; Crawford, M. K.; Grey, C. P.; Corbin, D. R. *Mater. Res. Soc. Symp. Proc.* **1995**, *376*, 751.
- (20) Grey, C. P.; Poshni, F. I.; Gualtieri, A. F.; Norby, P.; Hanson, J. C.; Corbin, D. R. *J. Am. Chem. Soc.* **1997**, *119*, 1981.
- (21) Olson, D. H. *Zeolites* **1995**, *15*, 439.
- (22) Chen, Y.; Paddison, S. J.; Tschinkow-Row. *J. Phys. Chem.* **1994**, *98*, 1100.
- (23) Böttcher, C. J. F. *Theory of Electric Polarisation*; Elsevier: New York, 1973; Vol. 1.